Journal of Machine Engineering, 2026, Vol. 26
ISSN 1895-7595 (Print) ISSN 2391-8071 (Online)

Received*: 11 September 2025* / Accepted: *16 February 2026* / Published online: *25 February 2026*

drilling process,
FEM thermal simulation,
chip removal,
optimum process conditions

Ikuo TANABE[1*]

DEVELOPMENT OF FEM SIMULATION TECHNIQUE FOR THE SEARCH OF OPTIMUM DRILLING PROCESS CONDITIONS

The requirements for machining include higher precision and productivity. To achieve these, measures against thermal deformation of machine tools and forced cooling of cutting heat are necessary. In recent years, there is also strong demand for energy-saving, resource-saving and environmentally friendly manufacturing in response to the SDGs and carbon neutrality. Under these conditions, it is an extremely difficult task to determine the optimum machining conditions while taking into account the need for high precision and improved productivity. In drilling, too, it is desired that the optimum drilling conditions can be determined instantaneously, but the variety of workpieces and drills makes it difficult to find the optimum drilling conditions for them. In this study, the FEM simulation technique that can calculate drill tip temperatures with high accuracy for the inputs of workpiece and drill materials, hole diameter and hole depth instructions and machining conditions (drill speed, feed rate, step feeding and forced cooling specification) in drilling was developed and evaluated in the experiment. The results showed that the proposed FEM simulation technique could calculate the drill edge temperature with high accuracy and quickly, easily. Therefore, it was effective as a tool for searching for optimum drilling conditions.

1. INTRODUCTION

The requirements for machining include higher precision [1, 2] and productivity. To achieve these, measures against thermal deformation of the machine tool [3–10] and forced cooling [11–14] of the cutting heat are necessary. In addition, the cutting of difficult-to-cut materials such as titanium alloys and nickel alloys, which are materials for aerospace industry parts [15], requires a large amount of cutting fluid and electrical energy for forced cooling [16, 17] as a measure against cutting heat. Furthermore, in recent years, there is a strong demand for manufacturing that is environmentally friendly, in response to the SDGs and carbon neutrality [18]. It has also been pointed out that wet machining using large amounts of cutting fluid has adverse effects on worker health and the global environment [19]. Under

[1] Technical and Management Engineering, Sanjo City University, Japan
[*] E-mail: tanabe@mech.nagaokaut.ac.jp
https://doi.org/10.36897/jme/218158

these conditions, it is extremely difficult to determine the optimum machining conditions while taking into account the need for high accuracy and improved productivity. In drilling, it is desirable to instantly determine the optimum drilling conditions, but the variety of workpieces and drills makes the search for these optimum drilling conditions difficult.

In this study, an FEM simulation technique is developed to instantly calculate the drill tip temperature in response to the inputs of workpiece and drill material, hole diameter and hole depth instructions, and machining conditions (drill speed, feed rate, step feeding and forced cooling specification) during drilling process. Specifically, first, a model for calculating the cutting heat generated on the drill tip during drilling process is constructed using cutting theory [20, 21]. Next, a technique is developed to calculate the maximum temperature change at the drill tip using the calculated cutting heat generation and FEM unsteady thermal deformation simulation. The dynamic drilling simulation is simulated by using FEM transient thermal simulation with the time-dependent heat generation, heat transfer coefficient and thermal conductivity in the static implicit software SOLIDWORKS 2023. This dynamic drilling simulation includes step feeding, forced cooling and chip removal, but not forced cooling by through-holes. Experiments are then carried out to evaluate the proposed FEM simulation technique and, finally, machining condition search considerations for productivity are also discussed. Note that these analyses are generally difficult to perform with static implicit FEM, which does not have the ability of remeshing or delete elements during the calculation.

2. BUILDING A MODEL OF CUTTING HEAT GENERATION DURING DRILLING PROCESS BY DIVERTING 2D CUTTING MODEL

In this chapter, a calculation model for cutting heat generation during turning is first developed using the two-dimensional cutting model cutting theory [20, 21]. The calculation model is then used to construct a calculation model for cutting heat generation during drilling process.

As shown in Fig. 1, a 2D cutting model is used to calculate the heat quantity Q_t [W]

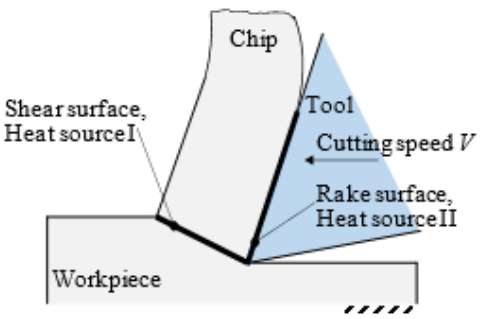

Fig. 1. Schematic view for 2-dimension cutting model

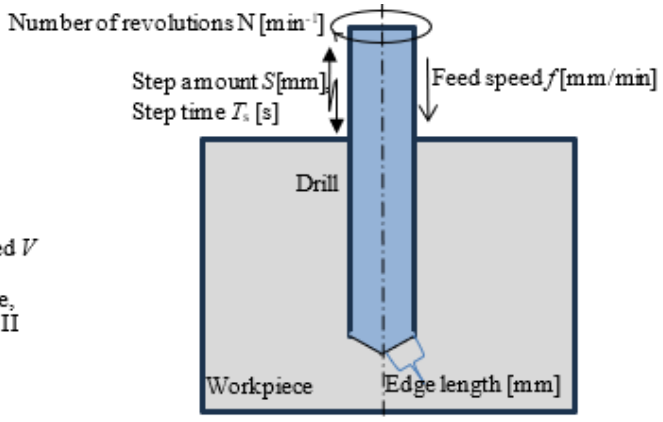

Fig. 2 Schematic view of the calculation models using the 2D cutting model for the drilling process

flowing into the tool, Q_w [W] into the workpiece and Q_c [W] into the chips from the machining conditions. The cutting heat is composed of three components: heat generated by the plastic deformation of the shear surface, frictional heat between the chip and the tool rake surface, and frictional heat between the tool relief surface and the workpiece. The frictional heat between the tool relief surface and the workpiece is small and will not be dealt with further in this study. The heat quantity Q_t [W] flowing into the tool is shown in Equation (1), the heat quantity Q_w [W] flowing into the workpiece is shown in Equation (2) and the heat quantity Q_c [W] flowing into the chip is shown in Equation (3) [20].

$$Q_t = q_f A_2 (1 - R_2) \tag{1}$$

$$Q_w = q_s A_1 (1 - R_1) \tag{2}$$

$$Q_c = q_s A_1 R_1 + q_f A_2 R_2 \tag{3}$$

Where, $$R_1 = \frac{1}{1+ [0.663 \cos\gamma / \sin\varphi \cos(\varphi - \gamma)] / \sqrt{\frac{V \cos\gamma}{4 k_c \sin\varphi \cos(\varphi - \gamma) / c_c \rho_c}}}$$

$$R_2 = \frac{\frac{bS}{2k_t} - \frac{\theta_s}{q_f}}{0.377 \sqrt{4 l \cos(\varphi - \gamma) / k_c c_c \rho_c V \sin\varphi \frac{bS}{2k_t}}}$$

$$\theta_s = \frac{k \sqrt{V t \sin\varphi \cos(\varphi - \gamma)}}{J_0 \sqrt{c_c \rho_c} (\sqrt{V t c_c \rho_c \sin\varphi \cos(\varphi - \gamma)} + 0.663 \sqrt{4 k_c}}$$

$$S = (2/\pi)\{(2l/b) \sinh^{-1}(b/2l) + \sinh^{-1}(2l/b) + b/6l + 1/3(2l/b)^2 - 1/3[(2l/b)^2 + \sqrt{1+(b/2l)^2}]\}$$

$$A_1 = b t / \sin\varphi , \; q_s = \frac{tbV [k\cos\varphi - \tau_s (\cot\varphi - 1)] [\cos\gamma / \cos(\varphi - \gamma)]}{J_0 b t \operatorname{cosec}\varphi}$$

$$A_2 = l b, \; q_f = \frac{k t b V \sin\varphi}{\sqrt{2} J_0 l} [1 + \sin(\gamma - \varphi)]$$

$$l = (t \tau_s / \tau_f)(\cos\gamma / \tan\varphi + \sin\gamma - 1)$$

$$\tau_s = k \tan\varphi / 1 + \tan\varphi, \; \tau_f = 0.3 \sigma G / E, \; \varphi = \pi/4 + \gamma/2 - \beta/2, \; \beta = \tan^{-1}\mu$$

where R_2 is the ratio of frictional heat at the rake surface flowing into the chip [-], A_1 is the area of the heated spot on the shear surface [m^2], A_2 is the area of the heated spot on the rake surface [m^2], q_f is the heating value per unit time and unit area at the rake surface [W/m^2], q_s is the heating value per unit time and unit area at the shear surface [W/m^2] and θ_s is the average temperature change of chips due to shear heat [K]. S is the shape factor [-], V is the cutting speed [m /min], t is the depth of cut [mm], b is the cutting width [mm], k is the specific cutting resistance [kgf/mm^2], γ is the rake angle [rad], φ is the shear angle [rad] and β is the friction

angle [rad]. k_c is the thermal conductivity of the chip [W/mK], c_c is the specific heat of the chip [J/kgK], ρ_c is the density of the chip [kg/m^3], σ is the tensile strength of the workpiece [Pa], E is Young's modulus [kgf/mm^2], G is the shear modulus [kgf/mm^2], μ is the friction coefficient [-], l is the rake surface contact length [m] and τ_s is shear stress [Pa], τ_f is the rake surface friction stress [Pa] and J_0 is the heat work equivalent [kgfm/J]. In addition to the machining conditions, the heat quantity flowing into the tool Q_t [W], the heat quantity flowing into the workpiece Q_w [W] and the heat quantity flowing into the chip Q_c [W] can be calculated by entering the physical properties of the workpiece and the friction coefficient into Equations (1), (2) and (3). The two-dimensional cutting model can be used as a calculation model for the cutting heat quantity during turning.

The drilling process shown in Fig. 2 is characterized by the fact that the cutting speed increases in proportion to the tool radius along the cutting edge from the center of the drill to the outer periphery. Here, the cutting speed V_r [m/s] on the cutting edge at 1/2 the drill radius in the 2D cutting model was used as the average cutting speed over the entire cutting edge length (constant value) to calculate the average temperature on the cutting edge. The average cutting speed of the drill, V_r [m/min], can be determined using Equation (4).

$$V_r = \frac{1}{2} \qquad V_D = \frac{\pi \ D \ N}{2 \times 1000} \tag{4}$$

Where V_D is the cutting speed of the drill [m/s], D is the drill diameter [mm] and N is the tool spindle speed [min^{-1}]. By inputting the average cutting speed of the drill, V_r [m/s], as the cutting speed V [m/s] in Equations (1), (2) and (3), the heat quantity Q_t [W] flowing into the drill, Q_w [W] flowing into the workpiece and Q_c [W] flowing into the chips can be calculated. The cutting width b [mm] uses the edge length in Fig. 2(b) and the depth of cut t [mm] uses the feed per drill revolution F [mm] in Equation (5).

$$F = f/2 \text{ N} \tag{5}$$

Where the denominator of 2 is for a two-blade drill and 1 for a one-blade drill. As shown in Table 1, the specifications of the workpiece, the tool and the hole are known at the preliminary stage of drilling process, and the machining conditions such as drill speed N [min^{-1}], feed rate f [mm/min], step amount S [mm], step time T_s [s] and forced cooling can be entered into Equations (1), (2), (3), (4) and (5). The heat quantity Q_t [W] entering the drill edge, Q_w [W] entering the workpiece and Q_c [W] entering the chips can finally be calculated.

Table 1. Explanations regarding parameters for the calculation of cutting calorific value

Tool and workpiece specifications	Machining specifications	Cutting condition
Workpiece; Material, Specific heat, Density, Specific cutting force, Young's modulus, tensile strength, thermal conductivity, shear modulus. Tool; Material, Thermal conductivity, rake angle, nose radius. ※Coefficient of friction between tool and workpiece.	Hole diameter Hole depth	Number of revolutions N [min^{-1}] Feed speed f [mm/min] Step amount S [mm] Step time T_s [s] Forced cooling [-]

3. ESTABLISH OF FEM SIMULATION TECHNIQUE FOR DRILLING PROCESS

3. 1. ALGORITHMS FOR NEW FEM SIMULATION TECHNIQUE

The drilling process is shown in Fig. 3. (a) shows the start of the next step process after the previous step process. (b) shows the end of drilling with a step amount of S [mm] and the generation of chips. (c) shows the drill being removed from the hole, chip removal, and forced cooling. In the drilling process, work is performed in the order (a) → (b) → (c) → (a) → (b) → (c) ・・・・ and drilling is continued until the desired depth is achieved. This step process is an important machining process for normal drilling.

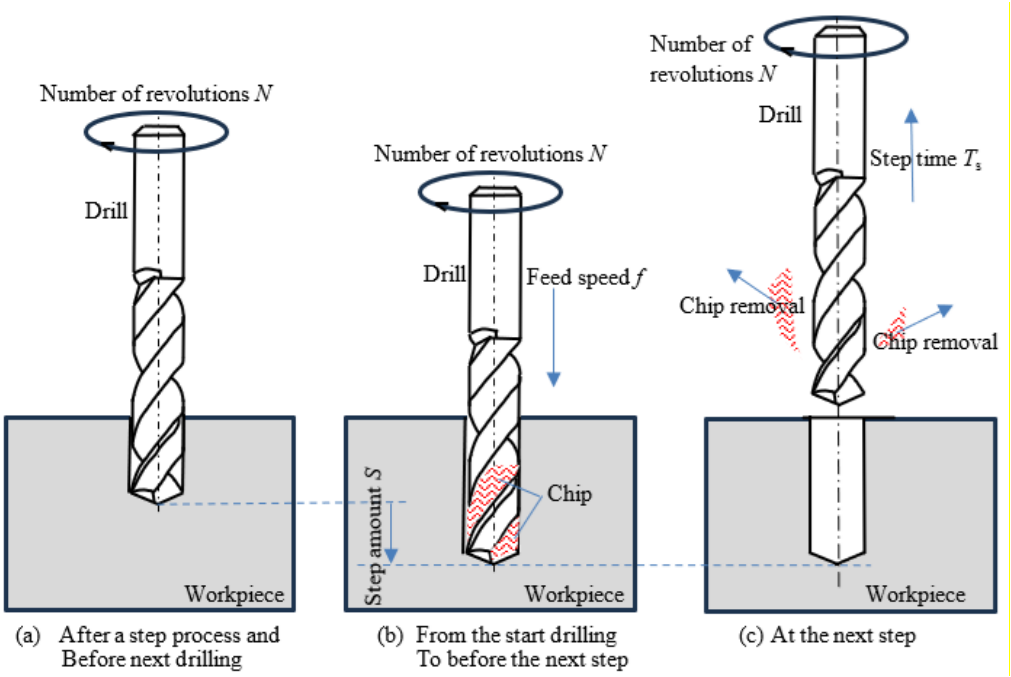

Fig. 3. Schematic view of the drilling process

A CAD model for searching optimal drilling conditions is shown in Fig. 4. The CAD model in Fig. 4 consists of four models: a drill model, a workpiece model, a chip model, and a step feed model. The model is at the end of the previous step process and the beginning of the next step feed (the first half of the step process, step amount *S* [mm]). The dynamic drilling process is simulated by FEM unsteady thermal analysis using only this FEM model. The chip removal and forced cooling process in the latter half of the step process is also performed using this CAD model. Thus, in this study, only the CAD model shown in Fig. 4 is used to perform coupled FEM transient thermal simulations of the drilling process in the first half of the step process and the chip removal and forced cooling processes in the second half of the step process. To simulate this dynamic drilling process with FEM transient thermal analysis, a step-feed model was added. A workpiece model and a drill model (Fig. 4) are firstly created, then a step-feed model is created based on these models using the cavity and the shell functions of the CAD software. The step feed element is made as thin as possible (0.25 mm

in this study) to increase the accuracy of the analysis and because it is a virtual model that is not originally needed. A chip model is finally created based on the step feed model using the cavity function of CAD. The length of chips ℓc [mm] generated by the step feed is calculated using Equation (6).

$$\ell c = \frac{S D^2 \pi}{4 A_c} \tag{6}$$

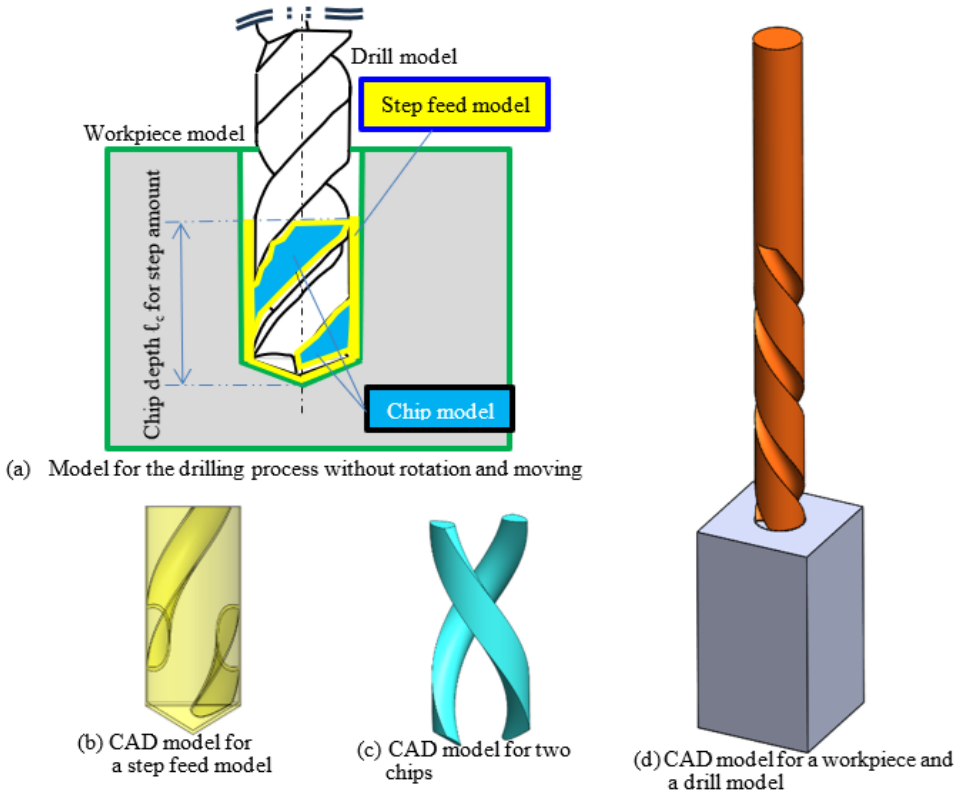

Fig. 4. Schematic view of the CAD models for searching of the optimum drilling process conditions

Where is the drill diameter D [mm], the chip cross-sectional area A_c [mm^2], and the step amount S [mm]. Table 2 shows the heat source, initial conditions, thermal properties, and thermal boundary conditions for the FEM simulation (unsteady thermal analysis) of the drilling process. These conditions are also divided into two processes: drilling and chip removal/forced cooling, which are repeated until the desired hole depth is achieved. For the heat source, the cutting heat value calculated in Chapter 2 was used for drilling, while the heat value during chip removal and forced cooling in the second half of the step-feed process was assumed 0 [W]. The heat source location is the edge of the drill model (edge width x rake surface contact length l, see Chapter 2) and the entire model for the chip model (the heat source is the sum of the heat inflow into the workpiece and chips). The overall heat generation in the chip model includes the heat generated by the removed workpiece and simulates, on average, the movement and heat conduction of chips along the drill groove during the drilling process. The initial condition is that the temperature of the entire model is set to 0 K only for the calculation of the first drilling process. For the coupled analysis, the model final temperature from the previous analysis is used as the initial condition. For the workpiece

model and the drill model, the physical properties of the actual workpiece and drill are used. For the thermal boundary conditions of the workpiece model and the drill model, the heat transfer coefficient corresponding to the part actually in contact with air or a cooling medium is set during the cutting process, and the heat transfer coefficient corresponding to the part actually in contact with air or a cooling medium during the chip removal and forced cooling processes is set. The chip model sets the heat transfer coefficient only on the top surface of the chip in contact with the air or cooling medium during the cutting process (the cooling effect is very small), sets the chip temperature to 0 K during the chip removal and forced cooling process, and sets the initial chip temperature in the FEM simulation to 0 K during the next cutting process. This simulates the chip removal behaviour. The step-feed model is set up so that the workpiece, drill, and chips are not in direct contact (like a buffer material), and continuous simulation of the drilling process and chip removal/forced cooling process is performed by setting the time-dependent thermal conductivity (details are described below in Section 3.2). As described above, FEM simulation (unsteady thermal analysis) can simulate drilling to a desired hole depth by repeatedly setting the heat source, initial conditions, thermophysical properties, and thermal boundary conditions shown in Table 2, while repeating the step processes (drilling process, chip removal, and forced cooling process) using the FEM model.

Table 2. Management of heat sources, thermal properties and thermal boundary conditions for FEM simulations regarding drilling process

<table>
<tr><th colspan="2">Simulated items</th><th>During drilling process</th><th>During chip removal and drill cooling</th><th>Next</th></tr>
<tr><td rowspan="4">Heat sources</td><td>Workpiece model</td><td>Nothing</td><td>Nothing</td><td rowspan="13">Repeat drilling and step process until drill tip temperature rise is steady</td></tr>
<tr><td>Drill model</td><td>Eq. (1) on the edge of Drill</td><td>Nothing</td></tr>
<tr><td>Chip model</td><td>Eq. (2) and Eq. (3) in Chip</td><td>Nothing</td></tr>
<tr><td>Step feed model</td><td>Nothing</td><td>Nothing</td></tr>
<tr><td rowspan="4">Initial condition</td><td>Workpiece model</td><td rowspan="4">Start time → 0 K,
From the second time onwards→ Temperature immediately after the step process</td><td rowspan="4">Only chip → 0 K,
Other →Temps. immediately after the drilling process</td></tr>
<tr><td>Drill model</td></tr>
<tr><td>Chip model</td></tr>
<tr><td>Step feed model</td></tr>
<tr><td rowspan="4">Physical properties</td><td>Workpiece model</td><td>Original value</td><td>Original value</td></tr>
<tr><td>Drill model</td><td>Original value</td><td>Original value</td></tr>
<tr><td>Chip model</td><td>Same to workpiece</td><td>Same to workpiece</td></tr>
<tr><td>Step feed model</td><td>Large thermal conductivity (No thermal resistance between workpiece and drill).
Other properties are same to workpiece.</td><td>Very small thermal conductivity (Insulation between workpiece and drill.)</td></tr>
<tr><td rowspan="4">Boundary conditions.</td><td>Workpiece model</td><td rowspan="2">Real heat transfer coefficient of areas in contact with air or cooling medium.</td><td rowspan="2">Real heat transfer coefficient of areas in contact with air or cooling medium.
Real heat transfer coefficient of areas in contact with the step feed model</td></tr>
<tr><td>Drill model</td></tr>
<tr><td>Chip model</td><td>Upper surface of the chip</td><td>Very large heat transfer coefficient (For a simulation of the chip removing)</td></tr>
<tr><td>Step feed model</td><td>Nothing</td><td>Nothing</td></tr>
<tr><td colspan="2">Chip removal</td><td>Chip removal times</td><td>Nothing</td></tr>
</table>

3. 2. CONSIDERATION OF STEP-FEED MODEL

The blue box in Table 2 shows how the thermal properties is set for the step-feed model. During the drilling process, the thermal conductivity of the step-feed model is extremely high (1000 W/mK is used in this study) to simulate direct contact between the workpiece, drill, and chips, and during the chip removal and forced cooling processes, the thermal conductivity of the step-feed model is extremely low (0.01 W/mK) to simulate that the workpiece, drill, and chips do not conduct heat to each other. This is an important model for FEM simulation (transient thermal analysis) using a static implicit FEM.

3. 3. CONSIDERATION OF FORCED COOLING

The green box in Table 2 shows how the thermal boundary conditions for forced cooling is set. In the case of forced cooling (cooling with large heat transfer coefficient) with air or a cooling medium during drilling process, the actual heat transfer coefficient is set where the workpiece and the drill are in contact with the air or cooling medium during the drilling process.

The actual heat transfer coefficient is a value that depends on the physical properties of the cooling medium and the wind and flow velocities. During the chip removal and forced cooling processes, the actual heat transfer coefficient is also set to the part of the entire workpiece and the entire drill that is in contact with the air or cooling medium. Again, the actual heat transfer coefficient is set to a value that depends on the physical properties of the cooling medium and the wind and flow velocities. During the chip removal and forced cooling process, the area near the drill tip is also in a forced cooling state, and if sufficient heat transfer coefficient and time can be set, this can have the effect of extending the life of the drill. These forced cooling simulations can be optimized by adjusting the machining conditions of the step-feed process.

3. 4. CONSIDERATION OF NATURAL CHIP REMOVAL DURING THE DRILLING PROCESS

The red box in Table 2 shows the natural chip removal points during the drilling process, although chip removal is also performed during the chip removal/forced cooling process in the latter half of the step-feed model in Section 3.2. The timing of chip removal depends on the workpiece material and drilling conditions. The heat supplied to chips during the drilling process is extremely large, and the timing of chip removal is an important factor in determining the maximum tool temperature rise.

Natural chip removal during the drilling process can be performed by resetting the chip temperature to 0 K, as in the previous step-feed model. This natural chip removal is also performed in the coupled analysis. In this case, the heat generation at the drill edge is continuous and the thermal conductivity of the step-feed model is small (0.01 W/mK is used in this study).

4. EVALUATION OF NEW FEM SIMULATION TECHNIQUE

4. 1. DRILLING PROCESS FOR EVALUATION (EXPERIMENT)

The experimental setup for evaluation is shown in Fig. 5. A ϕ 12 mm through-hole is drilled in the centre of a 30 mm square × 50 mm long, S55C material, and the temperature change values at three points on the side of the workpiece are measured using T-type thermocouples. The thermocouples are each composed of 0.5 mm copper wire and constantan wire, with a measurement temperature range of –200℃ to 300℃. This thermocouple is bonded to the workpiece using Aron Alpha (Cyanacrylate-based instant adhesive) adhesive and reinforced with silicone bond. The results of these measurements are compared with the FEM simulation results in Section 4.2. Table 3 shows the drilling process conditions for the evaluation experiments. Experiment No. 1 is the machining condition that is considered reasonable (based on preliminary experiments and opinions of skilled workers) based on the workpiece material and tool specifications used. Experiment No. 2 is the machining condition that is doubled the rotation speed, Experiment No. 3 is the machining condition that is doubled the feed rate, Experiment No. 4 is the machining condition that is used no step feed, and Experiment No. 5 is the machining condition that is used wet cutting with water-soluble cutting fluid. Through these experiments, the proposed new FEM simulation technique is examined and evaluated.

The temperature changes on the side of the workpiece were shown in Fig. 6 to 10. The chips after the drilling process were also shown in these figures. These experimental results are used to evaluate the analysis results in the next section.

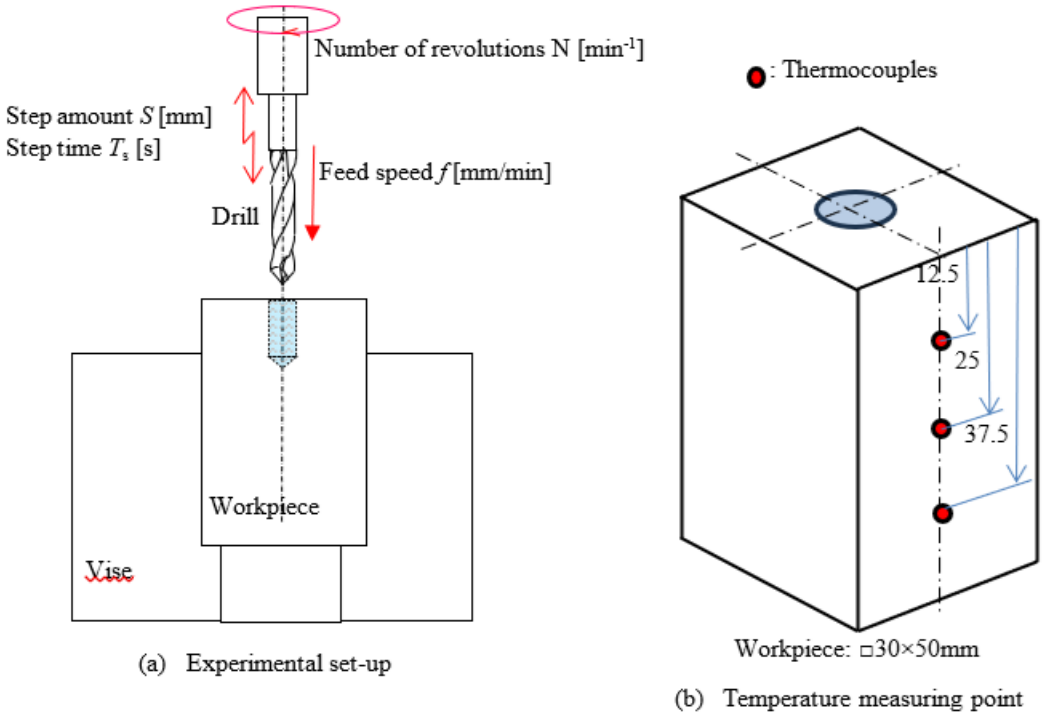

Fig. 5. Schematic view of the experimental set-up for evaluation experiment

Table 3. Cutting conditions for evaluation experiment

Experimental No.	**1**	2	3	4	5
Number of revolutions N [min^{-1}]	**1200**	2400	1200	1200	1200
Feed speed *f* [mm/min]	**240**	240	480	240	240
Step amount *S* [mm]	**12.5**	12.5	12.5	Continue	12.5
Step time T_s [s]	**0.2**	0.2	0.2	Nothing	0.2
Forced cooling [-]	**Without**	Without	Without	Without	With

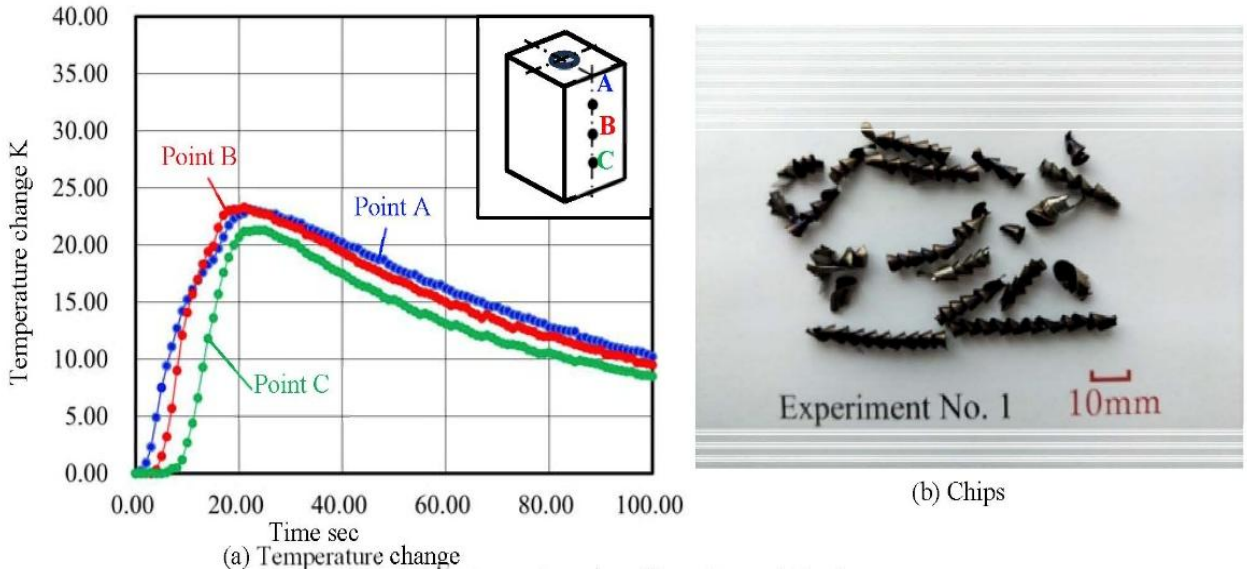

Fig. 6. Experimental results of Experimental No. 1

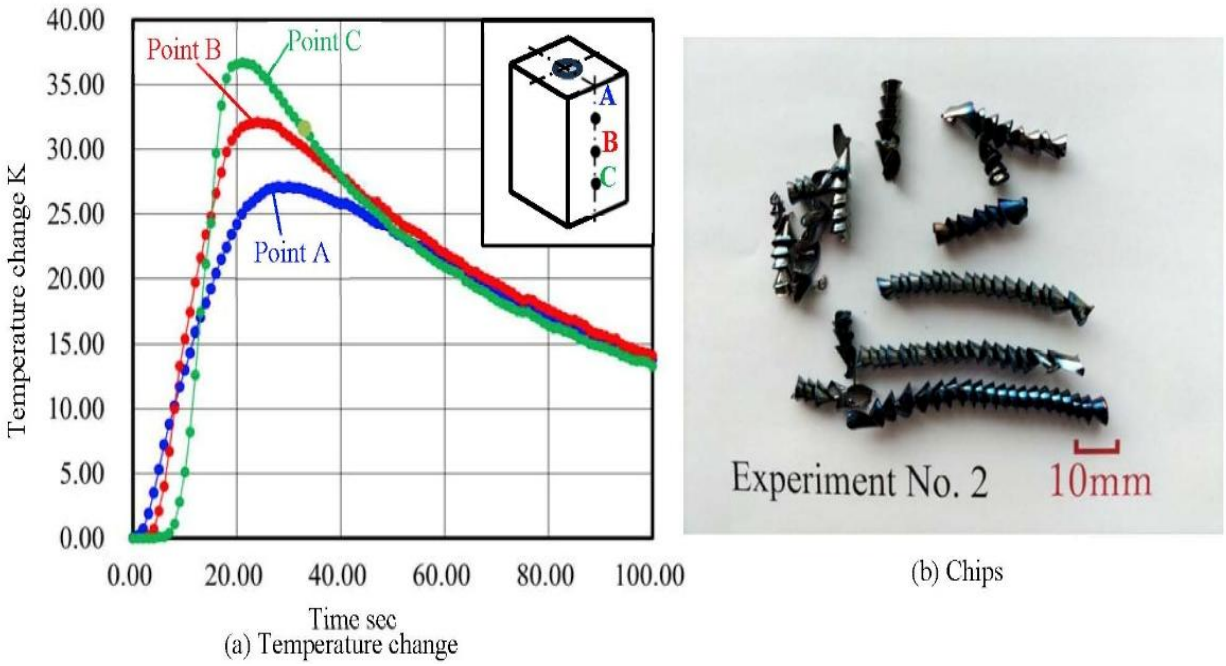

Fig. 7. Experimental results of Experimental No. 2

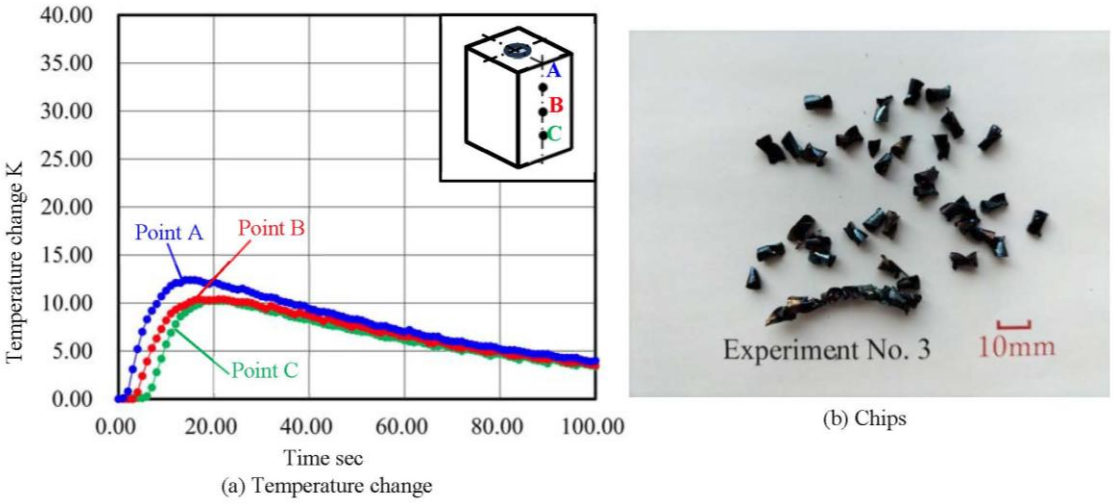

Fig. 8. Experimental results of Experimental No. 3

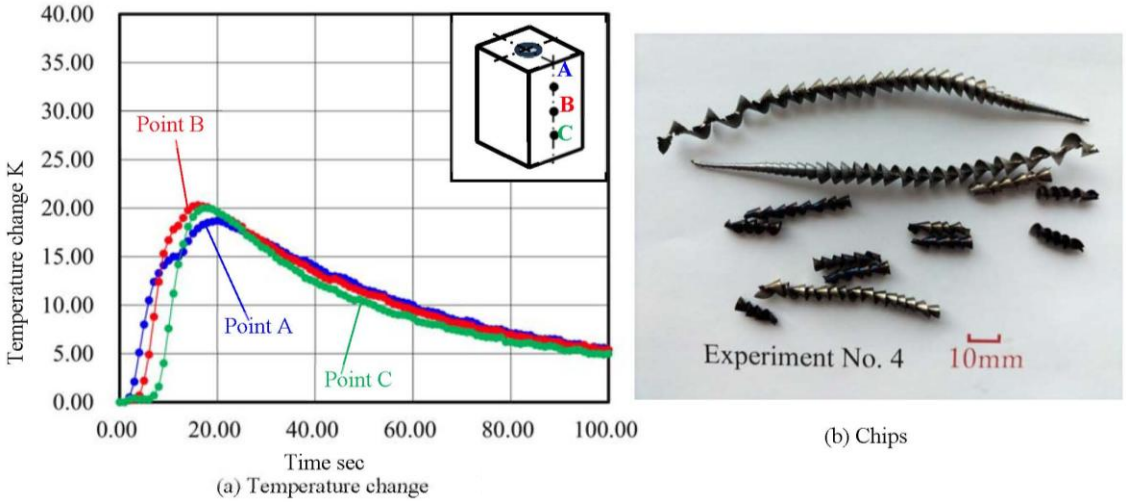

Fig. 9. Experimental results of Experimental No. 4

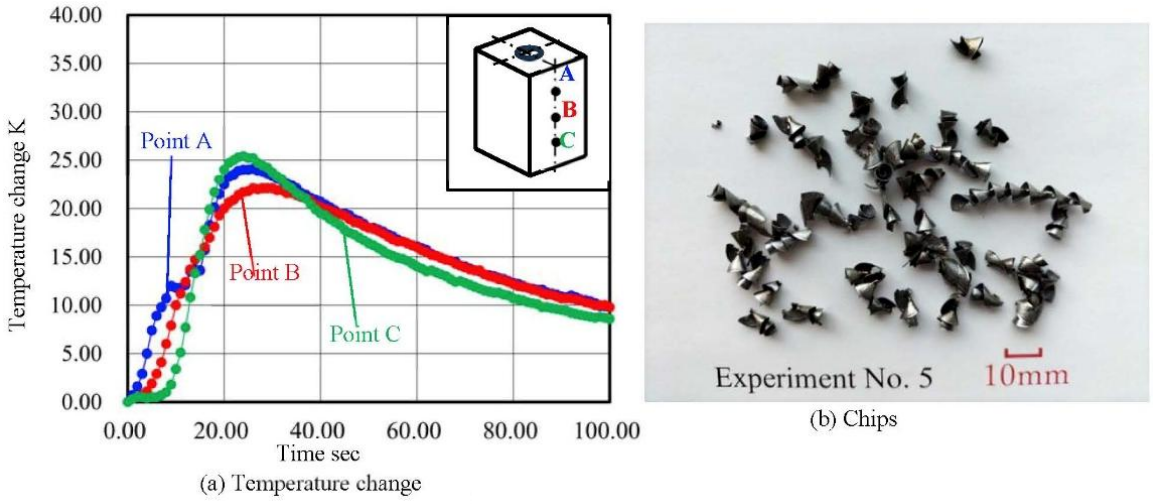

Fig. 10. Experimental results of Experimental No. 5

4. 2 EVALUATION OF NEW FEM SIMULATION TECHNIQUE (ANALYSIS)

Using the proposed new FEM simulation technique, an FEM simulation corresponding to the drilling experiment conducted in section 4.1 is performed. The FEM model corresponding to the evaluation experiment (See Figure 5) is shown in Fig. 11. The FEM model consists of four models: workpiece model, drill model, step feed model, and chip model, and has 15693 elements and 25821 nodes. Even when a mesh with twice as many elements is cut, the same level of calculation accuracy is confirmed, although it takes more calculation time. The analytical conditions for FEM simulations No. 1 (corresponding to Experiment No. 1), No. 2 (corresponding to Experiment No. 2), No. 3 (corresponding to Experiment No. 3), No. 4 (corresponding to Experiment No. 4) and No. 5 (corresponding to Experiment No. 5) are shown in Table 4, respectively. These analytical conditions were calculated using the calculation methods described in Chapters 2 and 3.

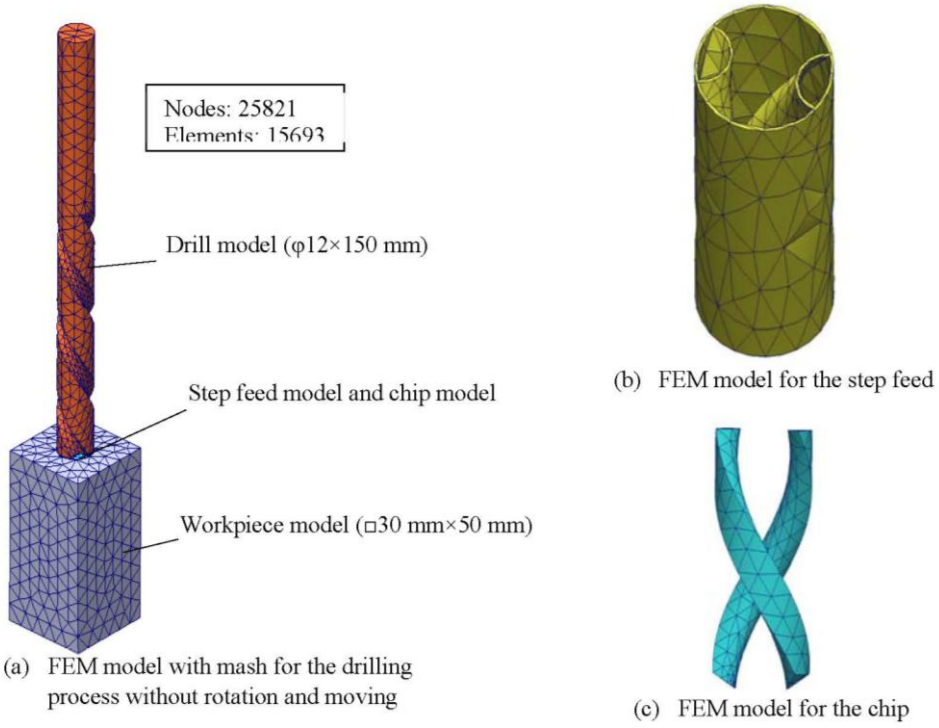

Fig. 11. Schematic view of the FEM models for searching of the optimum drilling process conditions

The analysis results of FEM simulation No. 1 are shown in Fig. 12. Figure 12 (a) shows the temperature distribution during the drilling process in the first step, Fig. 12 (b) shows the temperature distribution during chip removal in the first step. Fig. 12 (c) shows the temperature distribution at the end of the second drilling process, Fig. 12 (d) shows the temperature distribution immediately after chip removal and forced cooling in the second step, Fig. 12 (e) shows the temperature change in each part during the hole drilling process, and Fig. 12 (f) shows the temperature change on the side surface of the workpiece (experimental result No. 1 in Fig. 6(a) is also shown).

Table 4. Analysis conditions for evaluation FEM simulations regarding drilling process

FEM simulation No.1 for the Experimental No. 1				
Simulated items		During drilling process (Step amount 12 mm)	During chip removal and drill cooling (Step time 0.2 sec)	Next
Heat sources	Workpiece	Nothing	Nothing	Repeat drilling and step process until drill tip temperature rise is steady
	Drill	67 W×2, Arar (6.2 mm×0.46 mm×2 Edges)	Nothing	
	Chip	(267 W +436 W)×2	Nothing	
	Step feed	Nothing	Nothing	
Properties of Step feed model		Thermal conductivity: 1000 W/mk Other are same to workpiece.	Thermal conductivity:0.01W/mk Other are same to workpiece.	
Boundary conditio	Workpiece	15 W/m^{2}K, at air contact area	15 W/m^{2}K, at air contact area	
	Drill	15 W/m^{2}K, at air contact area	15 W/m^{2}K, at air contact area	
	Chip	15 W/m^{2}K, only upper surface	10000 W/m^{2}K at 0 K, only upper surface	
Process times		3.1 sec	0.2 sec	
Chip removal		2 times	Nothing	
FEM simulation No.2 for the Experimental No. 2				
Simulated items		During drilling process (Step amount 12 mm)	During chip removal and drill cooling (Step time 0.2 sec)	Next
Heat sources	Workpiece	Nothing	Nothing	Repeat drilling and step process until drill tip temperature rise is steady
	Drill	89 W×2, Arar (6.2 mm×0.46 mm×2 Edges)	Nothing	
	Chip	(436W + 1017 W)×2	Nothing	
	Step feed	Nothing	Nothing	
Properties of Step feed model		Thermal conductivity: 1000 W/mk Other are same to workpiece.	Thermal conductivity:0.01W/mk Other are same to workpiece.	
Boundary conditio	Workpiece	15 W/m^{2}K, at air contact area	15 W/m^{2}K, at air contact area	
	Drill	15 W/m^{2}K, at air contact area	15 W/m^{2}K, at air contact area	
	Chip	15 W/m^{2}K, only upper surface	10000 W/m^{2}K at 0 K, only upper surface	
Process times		3.1 sec	0.2 sec	
Chip removal		2 times	Nothing	
FEM simulation No.3 for the Experimental No. 3				
Simulated items		During drilling process (Step amount 12 mm)	During chip removal and drill cooling (Step time 0.2 sec)	Next
Heat sources	Workpiece	Nothing	Nothing	Repeat drilling and step process until drill tip temperature rise is steady
	Drill	108 W×2, Arar (6.2 mm×0.46 mm×2 Edges)	Nothing	
	Chip	(436 W +997 W)×2	Nothing	
	Step feed	Nothing	Nothing	
Properties of Step feed model		Thermal conductivity: 1000 W/mk Other are same to workpiece.	Thermal conductivity:0.01W/mk Other are same to workpiece.	
Boundary	Workpiece	15 W/m^{2}K, at air contact area	15 W/m^{2}K, at air contact area	
	Drill	15 W/m^{2}K, at air contact area	15 W/m^{2}K, at air contact area	
	Chip	15 W/m^{2}K, only upper surface	10000 W/m^{2}K at 0 K, only upper surface	
Process times		1.55 sec	0.2 sec	
Chip removal		7 times	Nothing	
FEM simulation No.4 for the Experimental No. 4				
Simulated items		During drilling process(Step amount 50 mm)		
Heat sources	Workpiece	Nothing		
	Drill	67 W×2, Arar (6.2 mm×0.46 mm×2 Edges)		
	Chip	(267 W +436 W)×2		
	Step feed	Nothing		
Properties of Step feed model		Thermal conductivity: 1000 W/mk, Other are same to workpiece.		
Boundary conditi	Workpiece	15 W/m^{2}K, at air contact area		
	Drill	15 W/m^{2}K, at air contact area		
	Chip	15 W/m^{2}K, only upper surface		
Process times		12.4 sec		
Chip removal		12 times		
FEM simulation No.5 for the Experimental No. 5				
Simulated items		During drilling process (Step amount 12 mm)	During chip removal and drill cooling (Step time 0.2 sec)	Next
Heat sources	Workpiece	Nothing	Nothing	Repeat drilling and step process until drill tip temperature rise is steady
	Drill	67 W×2, Arar (6.2 mm×0.46 mm×2 Edges)	Nothing	
	Chip	(267 W +436 W)×2	Nothing	
	Step feed	Nothing	Nothing	
Properties of Step feed model		Thermal conductivity: 1000 W/mk Other are same to workpiece.	Thermal conductivity:0.01W/mk Other are same to workpiece.	
Boundary conditions.	Workpiece	300 W/m^{2}K, at coolant contact area	300 W/m^{2}K, at coolant contact area	
	Drill	300 W/m^{2}K, at coolant contact area	300 W/m^{2}K, at coolant contact area	
	Chip	300 W/m^{2}K, only upper surface	10000 W/m^{2}K at 0 K, only upper surface	
Process times		3.1 sec	0.2 sec	
Chip removal		2 times	Nothing	

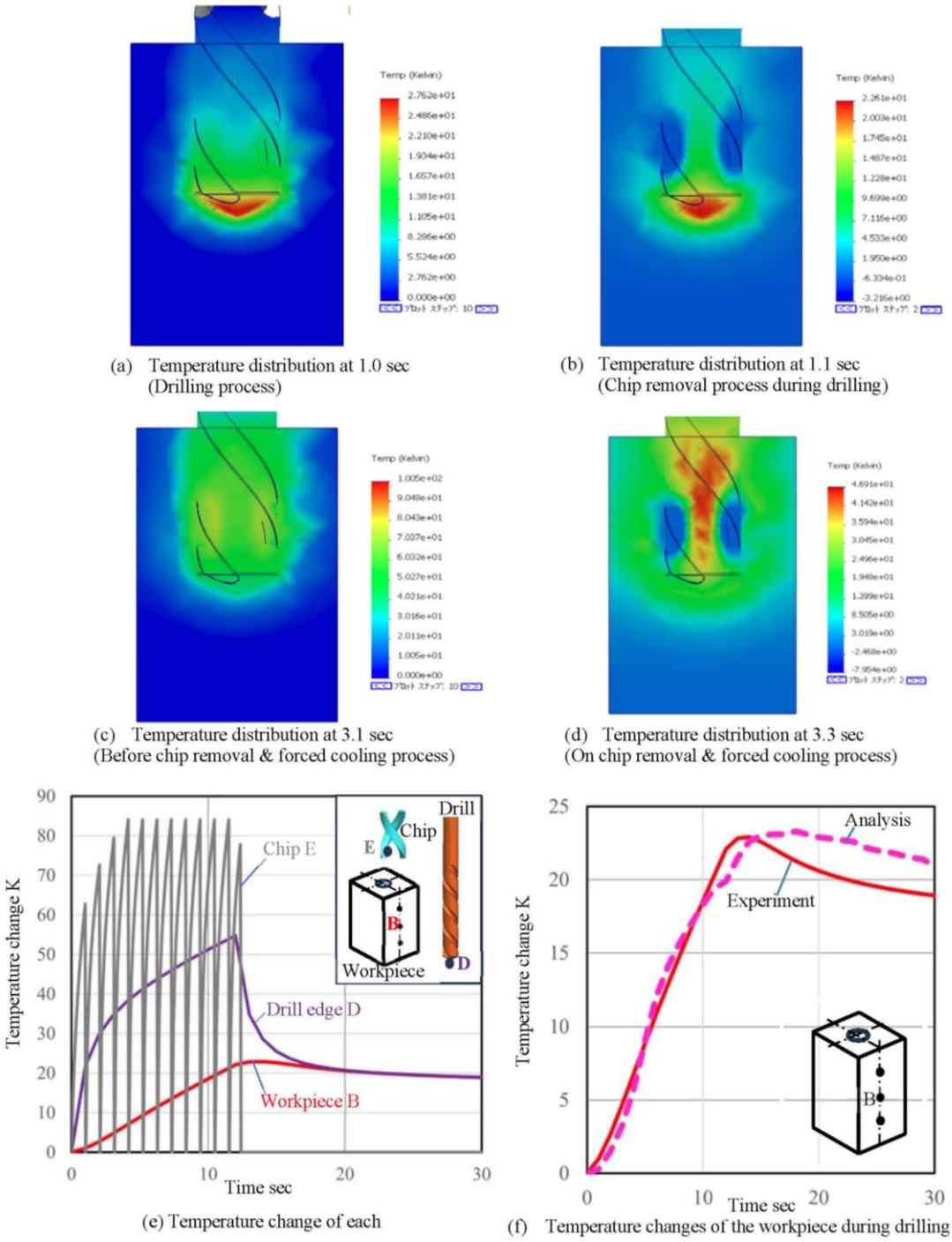

Fig. 12. Calculated results for FEM simulation No. 1

The step feed model and the algorithm for chip removal during the cutting process are functioning. The forced cooling algorithm is functioning, but the step time is too short to fully demonstrate its forced cooling capability. In Fig. 12 (f), even though the analytical model is a fixed model at a hole depth of 25 mm, a comparison of the temperature rise at point B shows that the analytical results correspond well to the experimental results, and the proposed drilling simulation technique is considered to be valid.

The analytical results of the maximum temperature change at point B of the workpiece for the five analytical conditions are shown in Figure 13. For evaluation purposes, the experimental results from Section 4.1 are also shown. The experimental and analytical results for No. 1, No. 2, No. 3, No. 4 and No. 5 all correspond accurately to each other, and the proposed new FEM simulation technique is considered to be effective for simulating drilling with a step feed process. These results confirm the validity of the cutting heat calculation model in Chapter 2, the validity of the proposed new FEM simulation technique, the validity and effectiveness of the step-feed model, and the effectiveness of the forced cooling and the validity of the calculations, respectively.

The results of the analysis of the maximum temperature change at the drill edge for the five analysis conditions are shown in Figure 14. It is possible to quantitatively determine the influence of the drilling process with and without step feed, the influence of the drilling process in the first half of the step feed, the influence of the chip removal and drill cooling process in the second half, and the influence of forced cooling, respectively.

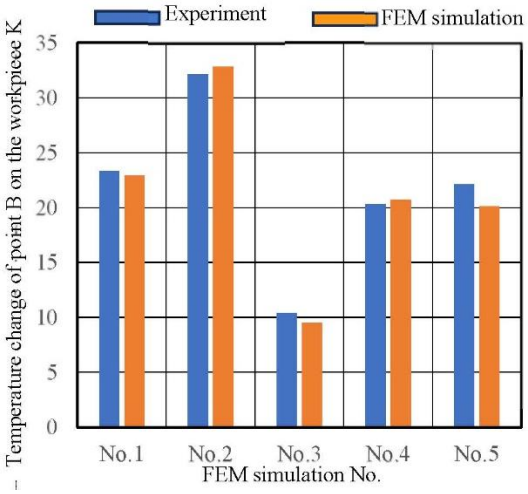

Fig. 13. Comparison of results between the experiments and the FEM simulations

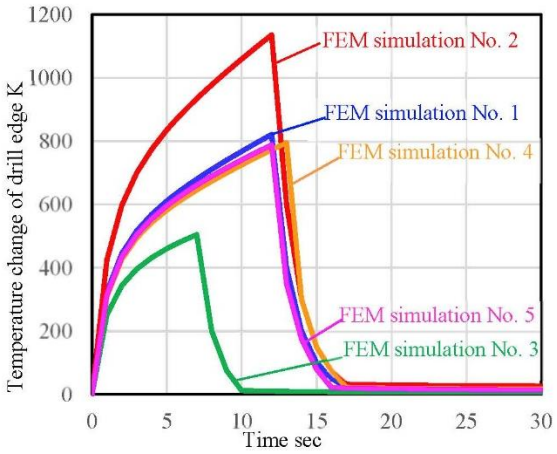

Fig. 14. Calculation results of the drill edge temperature using the FEM simulations regarding 5 analysis conditions.

As mentioned above, from Figs. 13 and 14, compared to the reference FEM simulation No. 1, the following can be said;

(a) FEM simulation No. 2 with doubled number of revolutions: the amount of cutting heat increased and the maximum drill edge temperature rise was more than 1100 K, well above the free-cutting temperature of carbide drills of 850 K.

(b) FEM simulation No. 3 with doubled feed speed: the machining time was reduced by half and the maximum temperature rise at the drill edge was suppressed to 500 K, regardless of the increase in cutting heat generation. This is a result of the high number of intermittent chip removals during drilling (seven times during one step process, see Table 7 and Fig. 8(b)) and the efficient removal of cutting heat generated.

(c) FEM simulation No. 4 without step feed: the maximum temperature change at the drill edge of No. 4 was somewhat lower than that of No. 1. This may be due to the fact that the number of chip removals in No.1 (10 times) was less than that in No.4 (12 times). It was also influenced by the fact that the forced cooling in No. 1 in the second half of the step process was short (0.2 s) and did not provide sufficient cooling effect.

(d) FEM simulation No. 5 with wet cutting with water-soluble cutting fluid: the effect of forced cooling with water-soluble cutting fluid was small. This was due to the indirect forced cooling during drilling in the first half of the step process and the short duration (0.2 s) of the forced cooling in the second half of the step process.

Thus, the proposed FEM simulation technique for drilling can be used to study in advance the optimum cutting speed, feed rate, step amount, step time and with/without forced cooling, and can be effectively used to search for optimum drilling conditions.

4. CONCLUSION

A new FEM simulation technique was developed and evaluated to find the optimum drilling process conditions. The results are summarized as follows; (1) In drilling process, a model was developed to calculate the cutting heat generated at the drill tip for the workpiece and drill material, hole diameter and hole depth instructions using cutting theory. (2) A new FEM thermal simulation accurately can calculate the maximum temperature change at the drill tip for the machining conditions of workpiece and drill material, hole diameter, hole depth, rotation speed, feed and step specification. (3) Using the proposed FEM simulation technology, it became possible to explore highly productive drilling conditions while considering drill tip temperature. (4) Using the proposed FEM simulation technology, it became possible to determine optimal step feed specifications (timing, step duration). Furthermore, as a future challenge, it is important to develop a method for FEM analysis of the timing of naturally occurring chips to improve the calculation accuracy of optimal step feed specifications.

REFERENCES

[1] GRZESIK W., 2020, *Modelling of Heat Generation and Transfer in Metal Cutting*, Journal of Machine Engineering, 20/1, 24–33, https://doi.org/10.36897/jme/117814.

[2] JEDRZEJEWSKI J., MODRZYCKI W., 2007, *Compensation of Thermal Displacement of High-Speed Precision Machine Tools*, Journal of Mechanical Engineering, 7/1, 108–114.

[3] BRECHER C., HIRSCH P., WECK M., 2004, *Compensation of Thermo-Elastic Machine Tool Deformation Based on Control Internal Data*, CIRP Annals – Manufacturing Technology, 53/1, 299–304.

[4] MARES M., HOREJS O., HORNYCH J., KOHUT P., 2011, *Compensation of Machine Tool Angular Thermal Errors Using Controlled Internal Heat Sources*, Journal of Machine Engineering, 11/4, 78–90.

[5] LANG S., ZIMMERMANN N., MAYR J., WEGENER K., BAMBACH M., 2023, *Thermal Error Compensation Models Utilizing the Power Consumption of Machine Tools*, S. Ihlenfeldt (Ed.), ICTIMT 2023, Springer, LNPE, 41–53, https://doi.org/10.1007/978-3-031-34486-2_4.

[6] MAYR J., JEDRZEJEWSKI J., UHLMANN E., DONMEZ M.A., KNAPP W., HÄRTIG F., WENDT K., MORIWAKI T., SHORE P., SCHMITT R., BRECHER C., WURZ T., WEGENER K., 2012, *Thermal Issues in Machine Tools*, CIRP Annals – Manufacturing Technology, 61, 771–791.

[7] PÖHLMANNP., MÜLLER J., Steffen IHLENFELDT S., 2024, *Strategy for Compensation of Thermally Induced Displacements in Machine Structures Using Distributed Temperature Field Control*, Journal of Machine Engineering, 24/3, 5–16, ISSN 1895-7595 (Print) ISSN 2391-8071 (Online).

[8] GEIST A., YAQOOB M. F., FRIEDRICH C., NAUMANN C., IHLENFELDT S., 2024, *Concept of Integrating a Hybrid Thermal Error Compensation Into an Existing Machine Tool Control Architecture*, Journal of Machine Engineering, 24/3, 32–46 ISSN 1895-7595 (Print) ISSN 2391-8071 (Online).

[9] TANABE I., SUZUKI N., ISHINO Y., ISOBE H., 2024, *Development of FEM Thermal Simulation Technology for Machine Tool with Enclosures and its Application*, Journal of Machine Engineering, 24/1, 17–28, ISSN 1895-7595 (Print) ISSN 2391-8071 (Online).
[10] BRECHER C., DEHN M. and NEUS S., 2023, *An Investigation of the Relationship Between Encoder Difference and Thermo-Elastic Machine Tool Deformation*, Journal of Machine Engineering, 23/3, 26–37, ISSN 1895-7595 (Print) ISSN 2391-8071 (Online).
[11] JEDRZEJEWSKI J., WINIARSKI Z., KWASNY W., 2020, *Research on Forced Cooling of Machine Tools and its Operational Effects*, Journal of Machine Engineering, 20/2, 18–38, https://doi.org/10.36897/jme/122769.
[12] MARES M., HOREJS O., FIALA S., HAVLIK L., STRITESKY P., 2020, *Effects of Cooling Systems on the Thermal Behaviour of Machine Tools and Thermal Error Models*, Journal of Machine Engineering, 20/4, 5–27, https://doi.org/10.36897/jme/128144.
[13] MARES M., HORES O., FIALA S., HAVLIK L. and STRITESKY P., 2020, *Effects of Cooling Systems on the Thermal Behaviour of Machine Tools and Thermal Error Models*, Journal of Machine Engineering, 20/4, 5–27, ISSN 1895-7595 (Print) ISSN 2391-8071 (Online).
[14] UHLMANN E., SALEINI S., POLTE M., TRIEBEL F., 2020, *Modelling of a Thermoelectric Self-Cooling System Based on Thermal Resistance Networks for Linear Direct Drives in Machine Tools*, Journal of Machine Engineering, 20/1, 43–57 ISSN 1895-7595 (Print) ISSN 2391-8071 (Online).
[15] TANABE I., ISOBE H., 2025, *Development of Forced Cooling Technology Using DIC Coating Tool with a Small Through-Hole and a Communicating Tube Regarding the Turning for Difficult-To-Machine Material*, Journal of Machine Engineering, 25/1, 45–56, ISSN 1895-7595 (Print) ISSN 2391-8071 (Online).
[16] SEKIYA K., YAMANE Y., NARUTAKI N., 2004, *High Speed End Milling of Ti-6Al-4V Alloy*, Journal of the Japan Society for Precision Engineer, 70/3, 438–442 (in Japanese).
[17] HAYASHI S., 2002, *Machining Super Alloys by Using Some Coolants in Different Applying Methods*, Journal of the Japan Society for Precision Engineer, 68/7, 438–442 (in Japanese).
[18] TANABE I., 2022, *Application of the Pentagonal W-Eco Model for Manufacturing Based on "SDGs",* Journal of Machine Engineering, 22/1, 25–42, ISSN 2391-8071 (Online)
[19] SATO U., TAKENOUCHI T., HARA H., YAMAZAKI AKABAYASHI S., 2004, *End Milling of Stainless Steel Using Electrolyzed Reduced Water*, Transactions of Japan Society of Mechanical Engineers, Series C, 72/718, 192–194 (in Japanese).
[20] HIRANO M., TERASHIMA A., HO Y.J., SHIRASE K., YASUI T., 1998, *Behaviour of Cutting Heat in High Speed Cutting*, Journal of the Japan Society for Precision Engineer, 64/7, 1067–1071 (in Japanese).
[21] TAKEYAMA, H., 1981, *Machining*, Maruzen Publishing Co., Ltd., 24–69 (in Japanese).